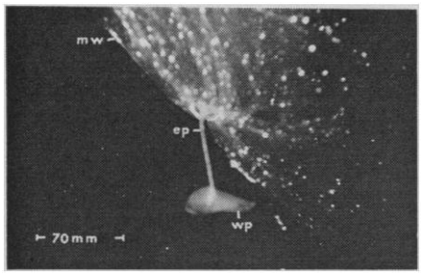

Fig. 3. *Gleba cordata* feeding from its delicate mucus web at a depth of 20 m in the Florida current. Only the tip of the extended proboscis (*ep*) touches the mucus web (*mw*) while the lateral grooves consolidate the particles entrapped in the mucus and move them toward the mouth. The wing plate is denoted *wp*.

(Fig. 3). When feeding, the animal is motionless below the web and assumes an inverted position with wings outstretched; an elongated proboscis supporting the mouth extends high above the body and maintains contact with the web. The animal and web sink slowly while feeding, the web either assuming a concave shape funneled toward the mouth or becoming convex and almost encircling the animal. Most webs measure 2 m in diameter.

The mucus web of *Corolla spectabilis* resembles that of *Gleba*. Also, *Corolla* assumes the same feeding position with the proboscis extended to touch the web floating high above the wings.

Large mucus glands, located along the periphery of the wing plate (Figs. 1 and 2), are contiguous with ciliary tracts that extend from the wings over the length of the proboscis and terminate distally in grooves surrounding the mouth (Fig. 1). The wing glands are primarily responsible for secretion of the web. The final strands of a freshly formed web are moved by cilia to the lateral grooves on the proboscis, so assuring contact during feeding between the mouth and the web.

A variety of phyto- and zooplankton, dominated by tintinnids and other protozoa less than 800 μm across, collect in the sinking webs of both species. Measurements on webs of *Gleba*, stained with azure A, reveal that most pores have areas less than 500 μm^2. The net can simply entrap many large particles, but smaller detritus and nannoplankton, observed to account for about 50 percent of the food, are evidently captured by adhesion to the mucus itself. Entangled particles are pulled toward the lateral grooves of the proboscis where they are consolidated into a fine mucus string by ciliary action. The string passes through the mouth into the esophagus and, although no radula is present, the food presumably moves through a muscular gizzard and is digested as in other ciliary-feeding pteropods (*4*).

Contrary to what Morton (*5*) suggests, *Gleba* and *Corolla* are exceedingly rapid swimmers. A feeding animal could sense my presence up to a meter away. The escape response first entails breaking the proboscis free of the web, whereupon several strokes of the fins flip the animal over so that the conch is dorsal and the retracted proboscis is aligned with the now ventral wing plate. Both species are capable of escape speeds of at least 45 cm/sec. Presumably, their high transparency, ability to sense turbulent motion, and swimming ability permit predator-avoidance when in the vulnerable feeding position.

Previous reports of mucus-web ciliary feeding have been limited to sessile organisms in which mucus traps attached to a substrate are periodically withdrawn and digested (*6*). The discovery that pteropods use an unsupported mucus web for filtering food particles from the open ocean adds a new mechanism to the array of feeding patterns already described for planktonic organisms.

Information such as this could only have been obtained by a diver making direct observations of live, undisturbed animals in their natural habitat. Traditional sampling programs have hidden the actual importance of many organisms which, although planktonic, can actively avoid nets. Consequently, population sizes as well as basic natural histories have been grossly misrepresented in the literature. *Gleba* and *Corolla* are only two examples of many previously obscure animals we have seen while diving in blue water.

RONALD W. GILMER
Department of Zoology, University of California, Davis 95616

References and Notes

1. J. J. Tesch, *Das Tierreich* (Lief 36) 1 (1913); *Dana Rep. Carlsberg Found.* **28**, 1 (1946); *ibid.* **30**, 1 (1948); K. Bonnevie, *Rep. "Michael Sars" N. Atl. Deep Sea Exped.* **3**, 1 (1913); A. L. Massy, *"Discovery" Rep.* **3**, 267 (1932); A. Pruvot-Fol, *Faune Fr.* **58**, 1 (1954); T. Tokioka, *Publ. Seto Mar. Biol. Lab.* **5**, 59 (1955); R. Wormelle, *Bull. Mar. Sci. Gulf Carib.* **12**, 95 (1962).
2. J. Meisenheimer, *Wiss. Ergeb. "Valdivia"* **9**, 1 (1905).
3. J. E. V. Boas, *Vidensk. Selsk. Skr. 6 Raekke naturvidensk. mathemat. Afd.* **4**, 1 (1886); P. Pelseneer, *Sci. Rep. "Challenger" Exped. Zool.* **23**, 1 (1888).
4. J. E. Morton, *J. Mar. Biol. Ass. U.K.* **33**, 297 (1954); S. van der Spoel, *Euthecosomata: A Group with Remarkable Developmental Stages (Gastropoda, Pteropoda)* (Noorduijn, Gorinchem, 1967); C. M. Yonge, *J. Linn. Soc. Zool.* **36**, 417 (1926).
5. J. Morton, in *Physiology of Mollusca*, K. Wilbur and C. M. Yonge, Eds. (Academic Press, New York, 1964), vol. 1, p. 405.
6. G. E. MacGinitie, *Biol. Bull.* **77**, 115 (1939); J. Morton, *Trans. Roy. Soc. N.Z.* **79**, 1 (1951).
7. I thank Drs. William M. Hamner and Milton Boyd of the University of California, Davis, and Dr. Carol M. Lalli of McGill University for their aid in preparing the manuscript. Work supported in part by NSF grant GB-22851, a grant from the National Geographic Society, and a John Simon Guggenheim fellowship to W. Hamner. Research carried out at the Lerner Marine Laboratory of the American Museum of Natural History, Bimini, British West Indies.

3 February 1972; revised 17 March 1972

Adaptation in Retinal Rods of Axolotl: Intracellular Recordings

Abstract. *Intracellular recordings of the late receptor potential from rods of isolated axolotl retinas revealed the existence of a dark adaptation mechanism that is independent of rod pigment regeneration. Response amplitude of individual rods was measured as a function of intensity both before and at various times after exposure to bleaching illumination. The rod sensitivity increased by at least 3 to 4 log units during a period of 15 to 25 minutes following the bleach. During this time rod pigment regeneration was either too small to be measured or was nonexistent in our preparation.*

When a retina is exposed to either an increase or a decrease in illumination, large changes in visual sensitivity (adaptation) occur. The dark adaptation that follows photopigment bleaching has been found to consist of two parts: (i) the fast or "neural" component and (ii) the slow or photochemical component, which depends on the concentration of unbleached photopigment, regardless of whether or not regeneration of the visual pigment takes place (*1*). The fast component is independent of both bleaching and regeneration of the visual pigments and until recently was assumed to result from synaptic interactions at the bipolar cell level (*2*).

Due to technical difficulties, previous adaptation experiments have been limited almost exclusively to the investigation of extracellularly recorded mass potentials, unit responses proximal to the receptors (mainly from ganglion

cells), and the psychophysical response. As a result, little is known about the adaptive properties of the first elements of the visual pathway—the individual rods and cones. [Techniques of recording from retinal receptor cells have been described (*3–5*).] However, indirect evidence supports the view that at least a portion of the fast change in sensitivity after termination of exposure to light is due to an adaptation mechanism at the receptor level. The evidence is threefold. (i) The experiments of Naka and Rushton (*6*) revealed that no correlation exists between the membrane potential and the log sensitivity of S potentials recorded during dark adaptation in retinas of cyprinid fish. In addition, Dowling and Ripps (*7*) demonstrated the similarity in the adaptation properties of ganglion cell responses, S potentials, and electroretinogram (ERG) b-wave in the skate retina (containing only rods). There was no apparent relation between the S-unit membrane potential and the cell's sensitivity during dark adaptation. So in the fish and in skate, dark adaptation apparently occurs distal to the origin of the S potential, in all probability in the receptors themselves. (ii) An adaptation that is independent of regeneration of visual pigment has been described recently for the isolated P_{III} component of the ERG (*8, 9*). This component is thought to be due almost entirely to extracellular current flow originating from the receptor cells (*10*). (iii) Evidence for the existence of fast adaptation at the receptor level is provided by psychophysical and electrophysiological experiments suggesting that an early stage of dark adaptation is mediated by a chemical (as opposed to a neural) process (*8, 9, 11, 12*).

The most straightforward method of determining the extent and nature of adaptation at the receptor level is to record from individual rods and cones. We demonstrated the existence of a substantial rod adaptation mechanism that is not linked to regeneration of the rod pigment.

We chose the axolotl *Ambystoma mexicanum* for our experiments because its retinal cells are unusually large and easily penetrated by a microelectrode. Pieces of isolated axolotl retina were placed, receptor side up, on squares of continually moistened paper at ambient temperature (24° ± 2°C). Microelectrodes filled with either 2*M* potassium chloride or 4*M* potassium acetate penetrated receptor cells at depths ranging from 5 to 80 μm below the distal receptor surface. Three sets of experiments confirmed that these responses were from receptor cells. (i) Procion yellow M4-RAN dye (*13*) injected into these cells was found in receptors when preparations were examined histologically. (ii) The size of the stimulus area had little effect on the amplitude of these responses, in contrast to the large effect of area on responses of S units (*3*), including those of axolotl. (iii) When the stimulus was a brief, intense flash, the early receptor potential could be recorded from within these cells (*14*). A series of equal-energy monochromatic stimuli at 430, 525, and 580 nm were used to establish which of the three known types of axolotl receptor (*15*) had been penetrated. Cones and "green" rods, with absorption maximums (λ_{max}) near 575 and 430 nm, respectively, were penetrated very infrequently and usually could not be recorded from for more than a minute or two. Penetrations of "red" rods (λ_{max} about 515 nm) were both more numerous and more stable.

In the fortuitous instances reported here we recorded from several red rod cells for 1 to 2 or more hours. This length of time was sufficient to (i) measure the threshold of the dark-adapted cell (0.5 mv criterion response) and the response amplitude as a function of intensity with 200-msec monochromatic stimuli of 525-nm wavelength, (ii) bleach approximately 45 to 50 percent of the red rod pigment by a 30-second exposure to white light, and (iii) record the subsequent sensitivity changes as a function of time following the bleach. The amount of photopigment bleached and the time course of photoproduct decay was determined spectrophotometrically (Shimadzu model MPR-50L) in parallel experiments on isolated retinas with the same bleaching source and geometry used for the electrophysiology (*16*). Under the bleaching conditions used, regeneration of rod pigment was not measurable (less than 5 percent).

The response of a typical red rod cell before and after a 45 percent bleach is shown in Fig. 1. Responses of the dark-adapted cell to a graded series of intensities from near-threshold to saturation were elicited (Fig. 1A). In Fig. 1B, the response to a stimulus of a single intensity is shown as a function of time after the bleach (*18*). During the bleach no response could be elicited from the cell with the highest stimulus intensity available (about 6.5 log units above the dark-adapted threshold). Ten seconds after extinction of the bleaching light, high-intensity stimulation produced a small, brief response (Fig. 1B). Gradually, both the amplitude and duration increased and in 15 to 20 minutes the receptor potential was qualitatively similar to the response before the bleach. However, photopigment bleaching reduced the amplitude of the saturated response (V_{max}) and shifted the response curve to the right (Fig. 1C), results indicating a decrease in sensitivity of the cell. Both before and after bleaching, the response amplitude as a function of intensity can be described by

$$V/V_{max} = I^n/(I^n + \sigma^n) \qquad (1)$$

where V is the peak response amplitude, I is the relative intensity, and σ is the half-saturation constant. Naka and Rushton (*19*) first used the simpler hyperbolic tangent function, where $n = 1$, to describe the relation of amplitude and intensity in fish S potentials. In the axolotl rods we studied, $n = 0.9 \pm 0.05$ (standard error), which is not inconsistent with $n = 1$. Others have reported values of n ranging between 0.7 and 1.0 (*5–7, 20*). After stabilization of sensitivity following a 45 to 50 percent bleach, σ had increased by 1.0 ± 0.1 log units. This shift in σ of 1 log unit agrees with the results of Ernst and Kemp (*9*), who reported that the light intensity required to produce a half-saturated P_{III} response increases tenfold after an approximately 50 percent bleach in the isolated rat retina, which contains nearly all rods. The mean ratio of V_{max} after a 45 to 50 percent bleach to V_{max} before the bleach was 0.53 ± 0.07. The recovery of sensitivity as a function of time after the bleach is also shown (Fig. 1C).

The averaged time course of change of rod threshold (0.5 mv criterion response) during the fast dark adaptation that follows a 45 to 50 percent bleach is shown in Fig. 2. After such a bleach the cell's sensitivity should be reduced but should not change as a function of time if (i) the sensitivity of the cell is related only to the concentration of unbleached photopigment and (ii) the photopigment is not being regenerated. These experiments illustrate that the rod sensitivity is influenced by a factor or factors other than rod pigment concentration. Although no measurable rod pigment regeneration occurred after a bleach, the sensitivity increased by at least 3 to 4 log units before stabilizing at about 1.5 log units above the dark-adapted threshold.

Superimposed upon the threshold

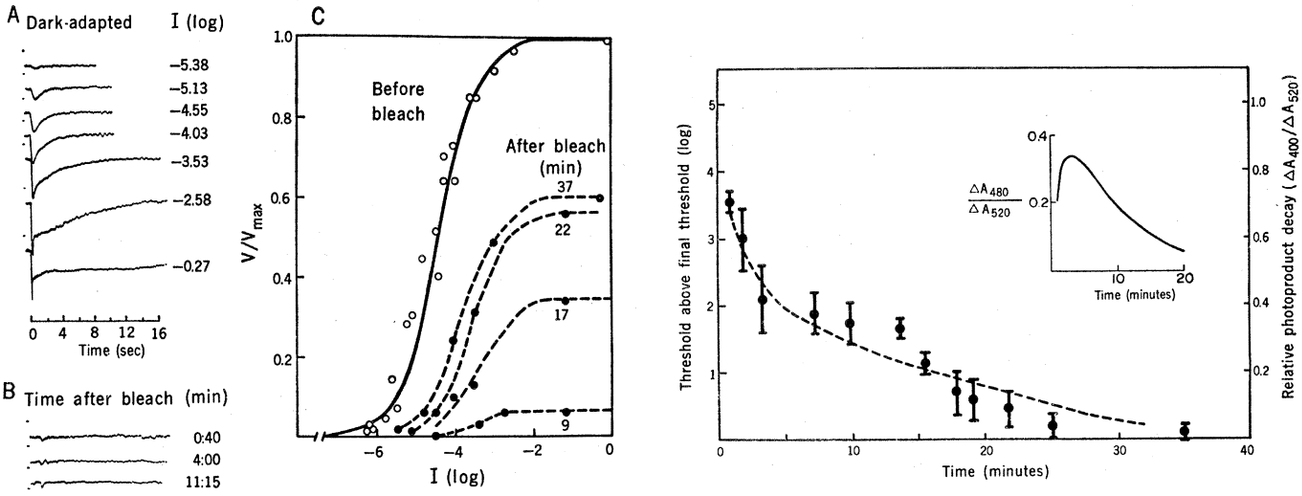

Fig. 1 (left). Intracellular responses of red rods to 200-msec light stimuli. The temperature was 25°C, and stimuli were presented at time 0. The cell was impaled 10 μm from the distal surface of the retina; the potential drop when the cell was penetrated was −30 mv. Downward deflection represents hyperpolarization. A 10-mv calibration pulse precedes each response. (A) Dark-adapted responses as a function of light intensity (I) are shown. (B) Responses to a stimulus of constant intensity (log I = −1.22) are shown for various times after a 45 percent bleach. (C) Curves of response amplitude (V) as a function of intensity were determined both before and after the bleach. The sold curve plots Eq. 1, where $n = 0.9$. Fig. 2 (right). Time course of dark adaptation and photoproduct decay. Solid circles are the mean log threshold for five cells as a function of time (error bars, ± 1 S.D.). The dotted line plots decay of absorbance (A) at 400 nm (mainly metarhodopsin II) and the inset shows photoproduct buildup and decay at 480 nm (metarhodopsin III). Both curves are the means of several determinations. Since both the amount of pigment bleached and the absorbance of each retina varied, the photoproduct data are normalized by dividing the change in absorbance at 400 and 480 nm by the total change in absorbance at 520 num (which is proportional to the amount of red rod pigment bleached). The bleach was presented between 0 and 30 seconds.

data in Fig. 2 is an averaged spectrophotometric curve obtained from whole isolated axolotl retinas; this curve shows the decay of absorption at 400 nm. Decrease in absorption at 400 nm during the first 20 minutes after a bleach is probably due mainly to decay of metarhodopsin II, one of the photoproducts resulting from bleaching of rhodopsin. The inset in Fig. 2 shows the buildup and decay of absorption at 480 nm, a measure of the concentration of metarhodopsin III or pararhodopsin (*16, 17*).

Donner and Reuter (*12*) showed the similarity in time courses of (i) decay of metarhodopsin II and (ii) the early portion of dark adaptation in the frog retina. Baumann and Scheibner (*21*) corroborated this finding. Ernst and Kemp (*9*) have indicated that the disappearance of another photoproduct (metarhodopsin III) may be linked to observed changes in isolated P_{III} amplitude during a "later" phase of fast dark adaptation. However, the involvement of either metarhodopsin II or III was discounted by Frank in frog (*8*) and by Frank and Dowling in rat (*17*); these experiments show different kinetics for adaptation as opposed to photoproduct decay. This controversy over the role of photoproducts in the process of dark adaptation cannot be fully resolved by our data. However, it seems clear that metarhodopsin III cannot be solely responsible for setting the rod sensitivity, since during the first few minutes absorbance at 480 nm initially increases rapidly and then decreases, whereas the log threshold is continually falling during this period. If decay of metarhodopsin II is accurately represented by decrease in absorbance at 400 nm, then the correlation between log sensitivity and metarhodopsin II concentration seems poor. However, the time course of absorbance decrease at 400 nm, especially in the later stages of photoproduct decay, is influenced by the presence of metarhodopsin III and possible accumulation of free retinal, both of which have absorption spectrums overlapping that of metarhodopsin II. The averaged data on log threshold suggest the presence of a plateau between 4 and 14 minutes. Some cells appeared to have a quite definite plateau while in others the log sensitivity smoothly increased in parallel with decay of absorbance at 400 nm. Further work is needed to determine whether or not these differences are due to experimental uncertainty (*22*).

Onset of the 30-second bleaching light resulted in maximum hyperpolarization of the cell's membrane potential; at offset of the bleaching stimulus, however, change in membrane potential was small or nonexistent. Unfortunately, the relation between membrane polarization and rod sensitivity could not be determined in most experiments. Generally, the observed membrane potential drifted slowly during the measurement period due to instabilities in the recording system. However, in two cases the rod membrane potential appeared to be exceptionally stable and free of random fluctuations both before and after the bleach. In these two cells slow repolarization of the membrane paralleled the log threshold decrease from 15 seconds to about 20 minutes following the bleach.

The possible existence of additional adaptation mechanisms involving more proximal cells is not excluded by our results, but the data presented here indicate that a substantial portion of the fast or "neural" adaptation process is observed in the photoreceptors.

S. R. GRABOWSKI
L. H. PINTO, W. L. PAK
Department of Biological Sciences,
Purdue University,
Lafayette, Indiana 47907

References and Notes

1. J. E. Dowling, *Nature* **188**, 114 (1960); W. A. H. Rushton, *J. Physiol. London* **156**, 193 (19(→ J. E. Dowling, *J. Gen. Physiol.* **46**, 1287 (1963).
2. J. E. Dowling, *Science* **155**, 273 (1967); G. W. Weinstein, R. R. Hobson, J. E. Dowling, *Nature* **215**, 134 (1967).
3. T. Tomita, *Cold Spring Harbor Symp. Quant. Biol.* **30**, 559 (1965).

4. F. S. Werblin and J. E. Dowling, *J. Neurophysiol.* **32**, 339 (1969).
5. D. A. Baylor and M. G. F. Fuortes, *J. Physiol. London* **207**, 77 (1970).
6. K. I. Naka and W. A. H. Rushton, *ibid.* **194**, 259 (1968).
7. J. E. Dowling and H. Ripps, *J. Gen. Physiol.* **56**, 491 (197 → *ibid.* **58**, 163 (1971).
8. R. N. Frank, *Vision Res.* **11**, 1113 (1971).
9. W. Ernst and C. M. Kemp, *ibid.*, p. 1197.
10. See K. T. Brown [*Vision Res.* **8**, 633 (1968)] for a review of ERG components and their origins.
11. W. A. H. Rushton and D. Spitzer, *J. Physiol. London* **218**, 101P (1971).
12. K. O. Donner and T. Reuter, *Vision Res.* **7**, 17 (1967).
13. A. O. W. Stretton and E. A. Kravitz, *Science* **162**, 132 (1968); A. Kaneko, *J. Physiol. London* **207**, 623 (1970); Procion yellow M-4RAN was obtained from ICI America.
14. M. Murakami and W. L. Pak, *Vision Res.* **10**, 965 (1970).
15. The axolotl has a mixed retina containing numerous red rods and a smaller number of green rods, cones, and double cones [M. Jonova, *Zool. Jahrb. Abt. Anat. Ontog. Tiere* **57**, 296 (1933); personal observations]. P. A. Liebman and J. H. Parkes gave us data from their unpublished microspectrophotometric experiments on outer segments from axolotl receptors. They found two types of rod outer segments: 85 to 90 percent were so-called red rods with λ_{max} at 505 to 516 nm, and 10 to 15 percent were green rods with λ_{max} at about 430 nm. One type of cone, with λ_{max} at about 575 nm, was also detected. In addition, Liebman and Parkes discovered that individual axolotl red rods apparently contain a variable mixture of photopigments based on vitamins A_1 and A_2.
16. The absorption spectrums of whole isolated axolotl retinas were measured from 370 to 750 nm both before and at various times after a portion of the photopigment was bleached. These spectrums reflect mainly the absorption changes in the red rods because the red rod pigment predominates in the axolotl retina. The absorption maximums of axolotl red rod pigment and its photoproducts tend to be shifted to somewhat higher wavelengths than those of rhodopsin and its corresponding photoproducts, presumably because axolotl red rods contain a mixture of rhodopsin (based on vitamin A_1) and porphyropsin (based on vitamin A_2) (*15*). By obtaining difference spectrums at various times after the bleach, we were able to recognize the presence of at least two photoproducts, with peaks at 400 and 480 nm, respectively. The spectral positions and time courses of buildup and decay of these two absorption peaks were compared with the λ_{max}'s and kinetics of the more thoroughly studied rhodopsin photoproducts from frog and cattle. This comparison suggests that the peaks at 480 and 400 nm are due mainly to the presence of metarhodopsins III and II, respectively. Unfortunately, both metarhodopsin II and a later photoproduct—free retinal, which is subsequently reduced to vitamin A—absorb maximally near 400 nm. However, the following considerations make it unlikely that the reduction of free retinal to vitamin A makes a major contribution to the decay of the 400 nm peak during the first 25 minutes after the bleach. (i) One-third of the total decrease in absorbance at 400 nm occurs in the first 3 minutes after the bleach. Concurrently, absorbance at 480 nm increases, that is, metarhodopsin III accumulates, a result consistent with the interpretation that the decrease in absorbance observed at 400 nm during this time interval is associated with the decay of metarhodopsin II to metarhodopsin III. In any case, very little accumulation of the later photoproduct, free retinal, is expected during the first 3 minutes. (ii) Subsequently, metarhodopsin III decays to free retinal, which is in turn reduced to vitamin A. The concentration of free retinal at any instant, and thus its contribution to the absorbance at 400 nm, will depend on the relative kinetics of its production and removal. If reduction of free retinal is slow in comparison with its production, the kinetics describing decay in absorbance at 400 nm should gradually change with time as metarhodopsin II concentration decreases and free retinal becomes the dominant photoproduct in this region of the spectrum. However, in isolated axolotl retina at 24°C decay of the 400 nm peak can be described by a single first-order process (half-time of decay, 11.5 minutes) from 4 to 22 minutes after the bleach. Thus it appears that free retinal is removed as soon as it is formed during this period. (iii) Finally, our argument that the absorbance decrease at 400 nm corresponds mainly to metarhodopsin II decay is strengthened by the observation that the time course of absorbance change at 400 nm in axolotl closely parallels those absorbance changes identified as due mainly to decay of metarhodopsin II in frog by C. Gedney and S. Ostroy [*Biochim. Biophys. Acta* **256**, 577 (1972)] and by R. N. Frank [*Vision Res.* **9**, 1415 (1969)] and in rat by Frank and Dowling (*17*).
17. R. N. Frank and J. E. Dowling, *Science* **161**, 487 (1968).
18. Light stimuli at various intensities were presented in random order. Near threshold, stimuli were presented at 10-second intervals. After a high-intensity, saturating stimulus a prolonged hyperpolarization is observed, and presentation of a second stimulus before membrane repolarization results in a greatly diminished response. For that reason, the interval between consecutive stimuli was extended to about 50 seconds after high-intensity stimulation.
19. K. I. Naka and W. A. H. Rushton, *J. Physiol. London* **185**, 536 (1966).
20. R. M. Boynton and D. N. Whitten, *Science* **170**, 1423 (1970).
21. Ch. Baumann and H. Scheibner, *Vision Res.* **8**, 1127 (1968).
22. Control experiments in dark-adapted retinas showed that when the membrane potential is stable, the sensitivity of the cell is also fairly stable (± 0.2 log units). Sudden or gradual changes in the cell's sensitivity were usually accompanied by corresponding erratic changes in the observed membrane potential. Therefore, if large, random fluctuations in the membrane potential occurred after a bleach, subsequent data were discarded.
23. We thank S. E. Ostroy for many helpful discussions and W. A. Cramer for the use of his Shimadzu spectrophotometer. Supported by PHS research grant EY 00033 and predoctoral fellowship GM 45860.

28 December 1971; revised 9 March 1972 ■

Chronic Effects of Osmotic Opening of the Blood-Brain Barrier in the Monkey

Abstract. *In the monkey, the blood-brain barrier and the blood-aqueous and blood-vitreous barriers of the eye can be opened by internal carotid perfusion of solutions of 2 molar urea in a way compatible with survival and, in some few cases, without detectable neurological deficits. Urea presumably acts by osmotically shrinking the endothelial cells of the cerebrovascular vessels and opening their tight junctions. The high incidence of brain necrosis with neurological sequelae after perfusion of urea by the present technique precludes the use of osmotic opening of the blood-brain barrier for pharmacotherapy at this time.*

The blood-brain barrier regulates brain homeostasis by controlling exchange of material between the intravascular fluid and the central nervous system (*1*). In short-term experiments on rabbits, this barrier can be opened reversibly for the passage of large molecules by exposure to concentrated solutions of electrolytes or relatively lipid-insoluble nonelectrolytes (*2*). The action of these substances on the barrier is consistent with the hypothesis that they osmotically shrink barrier cells (presumably the cells of the vascular endothelium) and open the tight junctions between them (*2*, *3*).

Since temporary barrier opening would be a useful tool to study barrier function and could have a possible clinical application for brain pharmacotherapy (*1*, *4*), we wanted to know the effect of osmotically induced barrier breakdown on long-term animal morbidity and mortality. Previous studies of barrier breakdown dealt with acute pathophysiology without being concerned with consequences on survival or neurological function (*1*, *5*). Perfusion of solutions of 2*M* (2 osmol) urea into the internal carotid artery of rabbits opens up the barrier reversibly to the Evans blue–albumin complex in short-term experiments (*2*). The monkey was chosen for long-term studies because a more meaningful neurological and behavioral examination is feasible. As in man and rabbit, the internal carotid arteries are distributed solely to the brain and do not anastomose with vessels from the external carotid system (*5*–*7*).

Twenty-eight monkeys (*Macaca mulatta*) weighing 3.5 to 5.5 kg were anesthetized with intravenous pentobarbital (20 to 30 mg per kilogram of body weight). The left external carotid, lingual, and thyroid arteries were ligated. The left common carotid was ligated caudally and catheterized for brain perfusion (*5*, *7*). To indicate barrier permeability, Evans blue dye (4 ml/kg; concentration being 2 g per 100 ml of saline) was injected intravenously. This quantity of dye is bound completely to blood albumin and does not normally cross the blood-brain barrier (*2*). In the first five monkeys, a 1-cm hole was trephined in the skull and the pia-arachnoid was exposed. The pial arterioles were observed under a dissecting microscope while a freshly prepared and filtered solution of 2*M* to 3*M* urea